

## Accepted Manuscript

Title: Self-assembled nanoformulation of methylprednisolone succinate with carboxylated block copolymer for local glucocorticoid therapy

Authors: Marat Kamalov, Trinh Đặng, Natalia Petrova, Alexander Laikov, Duong Luong, Rezeda Akhmadishina, Andrei N. Lukashkin, Timur Abdullin



PII: S0927-7765(18)30014-6  
DOI: <https://doi.org/10.1016/j.colsurfb.2018.01.014>  
Reference: COLSUB 9093

To appear in: *Colloids and Surfaces B: Biointerfaces*

Received date: 2-8-2017  
Revised date: 9-1-2018  
Accepted date: 10-1-2018

Please cite this article as: Marat Kamalov, Trinh Đặng, Natalia Petrova, Alexander Laikov, Duong Luong, Rezeda Akhmadishina, Andrei N.Lukashkin, Timur Abdullin, Self-assembled nanoformulation of methylprednisolone succinate with carboxylated block copolymer for local glucocorticoid therapy, *Colloids and Surfaces B: Biointerfaces* <https://doi.org/10.1016/j.colsurfb.2018.01.014>

This is a PDF file of an unedited manuscript that has been accepted for publication. As a service to our customers we are providing this early version of the manuscript. The manuscript will undergo copyediting, typesetting, and review of the resulting proof before it is published in its final form. Please note that during the production process errors may be discovered which could affect the content, and all legal disclaimers that apply to the journal pertain.

## Statistical summary

6 332 words (excluding references)

8 figures (6 figures + 2 double panels)

## Self-assembled nanoformulation of methylprednisolone succinate with carboxylated block copolymer for local glucocorticoid therapy

Marat Kamalov<sup>1</sup>, Trinh Đặng<sup>1</sup>, Natalia Petrova<sup>1</sup>, Alexander Laikov<sup>1</sup>, Duong Luong<sup>1</sup>, Rezeda Akhmadishina<sup>1</sup>, Andrei N. Lukashkin<sup>2</sup>, and Timur Abdullin<sup>1\*</sup>

<sup>1</sup>*Institute of Fundamental Medicine and Biology, Kazan (Volga Region) Federal University, 420008 Kazan, 18 Kremlyovskaya St., Russia*

<sup>2</sup>*School of Pharmacy and Biomolecular Sciences, University of Brighton, Brighton BN2 4GJ, UK*

\*Corresponding author. E-mail: tabdulli@gmail.com (T. Abdullin).

## Graohical abstract



## Highlights

- Structure and concentration dependent association of EO/PO copolymers with amphiphilic solutes
- Self-assembly of methylprednisolone succinate (MPS) with EO/PO copolymers in aqueous solutions
- *In situ* MPS nanoformulation with increased antiradical activity and cellular availability
- Tandem mass spectrometry (MRM) analysis of MPS nanoformulation in biological samples

## ABSTRACT

A new self-assembled formulation of methylprednisolone succinate (MPS) based on a carboxylated trifunctional block copolymer of ethylene oxide and propylene oxide (TBC-COOH) was developed. TBC-COOH and MPS associated spontaneously at increased concentrations in aqueous solutions to form almost monodisperse mixed micelles (TBC-COOH/MPS) with a hydrodynamic diameter of 19.6 nm, zeta potential of  $-27.8$  mV and optimal weight ratio  $\sim 1:6.3$ . Conditions for the effective formation of TBC-COOH/MPS were elucidated by comparing copolymers and glucocorticoids with different structure. The micellar structure of TBC-COOH/MPS persisted upon dilution, temperature fluctuations and interaction with blood serum components. TBC-COOH increased antiradical activity of MPS and promoted its intrinsic cytotoxicity *in vitro* attributed to enhanced cellular availability of the mixed micelles. Intracellular transportation and hydrolysis of MPS were analyzed using optimized liquid chromatography tandem mass spectrometry with multiple reaction monitoring which showed increased level of both MPS and methylprednisolone in neuronal cells treated with the formulated glucocorticoid. Our results identify TBC-COOH/MPS as an advanced *in situ* prepared nanoformulation and encourage its further investigation for a potential local glucocorticoid therapy.

**Keywords:** methylprednisolone succinate; ethylene oxide and propylene oxide copolymers; nanoformulation; self-assembly; mixed micelles; cellular availability; mass spectrometry; local glucocorticoid therapy

## 1. Introduction

Glucocorticoids are adrenal cortex derived, natural and semisynthetic steroid hormones with pleiotropic biological activities in mammals [1]. They include cortisol (hydrocortisone), a primary endogenous hormone, and a range of its synthetic derivatives, such as dexamethasone, prednisolone, methylprednisolone and their ethers. Glucocorticoids are one of the most frequently used therapeutics with versatile effects on metabolic processes, pronounced anti-inflammatory, immunomodulatory, anti-allergic and anti-edema properties [1].

Besides routine use of glucocorticoids to treat widespread diseases, including allergies, asthma, autoimmune and degenerative disorders [1], they are also considered as emergency drugs administered in severe clinical cases, such as sepsis and acute neuronal traumas [2,3]. Methylprednisolone infusion therapy has been intensively studied in order to alleviate the consequences of acute spinal cord injuries which result from glutamate neurotoxicity and inflammation [3,4]. The neuroprotective action of glucocorticoids administered after hypoxia or traumatic injury was established [4–6]. This therapeutic effect is, however, observed within a relatively narrow range of concentrations, and increased drug levels could promote tissue degeneration [7].

The high therapeutic potential of glucocorticoids is accompanied by their intrinsic side effects, including immunosuppression, hypertension, osteoporosis, metabolic disturbances as well as decreased sensitivity upon repetitive administration [1]. Development of pharmaceutical approaches for reduction of these adverse effects is of considerable biomedical interest. The common strategy relies on the systemic use of glucocorticoids encapsulated into liposomal or micellar nanocarriers designed for increasing solubility and pharmacokinetic profile of the drugs [6,8]. Localized delivery of glucocorticoids to target tissues could provide substantial advantages over systemic administration. The advantages are related to improved safety and sustained therapeutic dose level. Localized therapy should be based on an effective delivery system, incorporating medical devices, carriers and/or penetration enhancers. The delivery systems are mainly designed to increase local bioavailability of a drug and promote its sustained release in the target tissues.

To date, various (bio)materials and strategies have been proposed for local delivery of glucocorticoids to pulmonary [9–11], ocular [12–15], inner ear [16], and neural [17] tissues.

Stable unilamellar vesicles composed of polysorbate 20, cholesterol and beclomethasone dipropionate were prepared by means of solvent evaporation and hydration methods. The resultant liposome-like vesicles were tested as a spray formulation to treat asthma and chronic obstructive pulmonary disease. The formulation penetrated with greater efficiency across the mucous layer, and exhibited increased cellular uptake and anti-inflammatory activity on human lung fibroblasts *in vitro* [9,10].

Ocular formulations of glucocorticoids developed to date include a covalent conjugate of polyamidoamine dendrimer with fluocinolone acetonide for intravitreal injection upon age-related macular degeneration [12]; a drop formulation of polymer-stabilized hydrocortisone nanosuspension with increased stability and sustained action [13]; budesonide-loaded polylactide nano- and microparticles with sustained release, anti-inflammatory and anti-VEGF properties for treatment of vascular disorders of the retina [15].

The main approaches for local delivery of glucocorticoids into the inner ear are based on injection of polymeric hydrogels onto the round window [16]. Thermoresponsive *in situ* forming hydrogel containing 20% Poloxamer 407 (Pluronic F127) and 30% triamcinolone acetonide has been recently developed for prolonged intratympanic release of the drug [18]. The formulation was shown to be tolerable and support therapeutic concentrations of triamcinolone acetonide in the perilymph over 10 days in a guinea pig model [19]. Intratympanic formulations of dexamethasone composed of Poloxamer 407 [20] and hyaluronic acid as a gelling agent [21] were also developed.

Whereas the reported local delivery systems include conventional particle and hydrogel based materials, less attention has been paid to usage of penetration enhancers in glucocorticoid therapy. Such enhancers could promote drug transportation across coverings of organs and tissues, thus permitting reduction of doses and side effects. In association with that, amphiphilic polymers such as copolymers of ethylene oxide (EO) and propylene oxide (PO) are promising materials with regulated physicochemical properties. The copolymers combine the ability to encapsulate different drugs and promote their intracellular and tissue transportation [22,23].

We have shown recently that glycerol based trifunctional block copolymers (TBCs) of EO/PO subjected to succinylation [24] or chemical oxidation [25] possessed enhanced cell membrane-modulating properties and biocompatibility. The oxidized TBC substantially promoted intraspinal delivery of rhodamine 123 as a model compound when applied onto

the open spinal cord of a rat [25]. In this study, we developed a novel self-assembled micellar nanoformulation of the TBC with methylprednisolone succinate, which is of particular interest in local therapy of inflammation related and traumatic diseases.

## 2. Materials and methods

### 2.1. Materials

Dexamethasone (Sigma-Aldrich), methylprednisolone sodium succinate (Metypred, OrionPharma) and methylprednisolone (Medrol, Pfizer) were used. 3-(4,5-dimethyl-thiazol-2-yl)-2,5-diphenyltetrazolium bromide (MTT), 2',7'-dichlorofluorescein diacetate, Triton X100, phenylmethanesulfonyl fluoride (PMSF), menadione sodium bisulfite were produced by Sigma-Aldrich. Pyrene, chromium (VI) oxide, reagents/solvents for chemical synthesis, and inorganic salts were purchased from Acros Organics. Hypergrade acetonitrile for LC-MS and formic acid were purchased from Merck Millipore.

Materials for cell culturing were obtained from PAA Laboratories. Milli-Q grade water (Milli-Q Advantage A10, Merck Millipore) was used to prepare buffers and solutions.

### 2.2. Copolymers of ethylene oxide and propylene oxide

Linear block copolymers of EO and PO, i.e. Pluronic L61, L121, F127 (trademark of BASF) were purchased from Sigma-Aldrich. Trifunctional glycerol-based EO/PO block copolymer Laprol 6003-2B-18 (TBC) (analogue of Voranol, Dow Chemical) was obtained from PJSC 'Nizhnekamskneftekhim' (Russia). The main physicochemical characteristics of the copolymers including the number-average molecular weight (MW), mean number of EO (x) and PO (y) units, the hydrophilic-lipophilic balance (HLB) [26] and the critical micellar concentration (CMC) values are shown in Table 1S (SM). TBC was chemically oxidized with the use of chromium oxide as recently described [25].

### 2.3. Preparation and characterization of copolymer-glucocorticoid compositions

Stock solutions of the copolymers were prepared in milli-Q water at a concentration of 10 mg/mL. Methylprednisolone succinate (MPS) was dissolved in isotonic sodium chloride solution (0.9%) at a concentration of 62.5 mg/mL (125.9 mM) recommended for infusion. MP and dexamethasone (DXM) were initially dissolved in DMSO.

To prepare compositions and mixed micelles composed of the glucocorticoids and copolymers, equal volumes of solutions of these two components were carefully mixed and left for 30 min to allow drug-copolymer association and mixed micelles formation.

Compositions of glucocorticoids and copolymers were characterized by a dynamic light scattering (DLS) technique on a Zetasizer Nano ZS analyzer (Malvern Instruments). The hydrodynamic diameter (HD), the particle dispersion index (PDI) and the zeta potential ( $\zeta$ -potential) of pure copolymers and their mixtures with drugs were determined. The HD and PDI were measured in an isotonic solution, PBS (pH 7.4) or twice diluted DMEM cell culture medium at different temperatures (25, 37 and 50°C).  $\zeta$ -potential was registered in 0.05 M HEPES buffer (pH 7.0).

Mixed micelles of TBC-COOH and MPS were characterized with the use of pyrene fluorescent probe as described elsewhere [27].

#### 2.4. Atomic force microscopy

TBC-COOH/MPS micelles were diluted with milli-Q water at final concentrations from 0.3 to 1.0 mg/mL (TBC-COOH) and from 2.1 to 6.3 mg/mL (MPS). Mica sheet was cut and cleaved into thin sections (1×1 cm) with the internal side used as a substrate. Aliquots (1  $\mu$ L) of TBC-COOH/MPS or TBC-COOH solutions were spread onto the substrate and air-dried. Atomic force microscopy (AFM) analysis was performed on a Bruker Dimension FastScan microscope (Bruker). The AFM images were obtained in PeakForce QNM (quantitative nanomechanical mapping) mode with the use of standard silicon cantilevers ScanAsystAir (Bruker) having curvature 2 nm and stiffness 0.4 N/m. Height profiles of typical nanostructures in AFM images and average geometry of the particles were presented (mean $\pm$ SD, n $\geq$ 20).

#### 2.5. Mammalian cell culturing

SH-SY5Y human bone marrow neuroblastoma and PC-12 rat pheochromocytoma (ATTC) cell lines were used. The cells were cultured aseptically in DMEM containing 10% fetal bovine serum (FBS), 2 mM L-glutamine, 100 U/mL penicillin and 100  $\mu$ g/mL streptomycin at 37°C in humidified air atmosphere with 5% CO<sub>2</sub>.

## 2.6. Assessment of antiradical properties of TBC-COOH/MPS

### 2.6.1. Fluorescent assay for Co/H<sub>2</sub>O<sub>2</sub> reaction

Stock solutions of cobalt chloride (CoCl<sub>2</sub>) and hydrogen peroxide (H<sub>2</sub>O<sub>2</sub>) were prepared in milli-Q water. H<sub>2</sub>O<sub>2</sub> concentration was verified spectrophotometrically at  $\lambda=240$  nm using an extinction coefficient of 43.6 M<sup>-1</sup>. CoCl<sub>2</sub> and H<sub>2</sub>O<sub>2</sub> were mixed in PBS (pH 7.4) to obtain final concentrations of 0.23 mM (CoCl<sub>2</sub>) and 21.6 mM (H<sub>2</sub>O<sub>2</sub>). 2',7'-dichlorofluorescein diacetate (DCFDA) was added at concentration of 5  $\mu$ M as a fluorescent indicator of oxygen radicals [28]. The reaction was carried out at ambient temperature in a 96-well plate with or without drug formulations. The fluorescence intensity was registered kinetically at  $\lambda_{\text{ex}}=488$  nm and  $\lambda_{\text{em}}=535$  nm during 60 min on an Infinite M200 PRO microplate analyzer (TECAN). The response to MPS and TBC-COOH/MPS was measured as a percentage of the signal of control Co/H<sub>2</sub>O<sub>2</sub> reaction without effectors (100%).

### 2.6.2. Fluorescent analysis of H<sub>2</sub>O<sub>2</sub>-induced oxidative burst in cells

PC-12 cells were seeded in a 96-well plate and allowed to form a confluent monolayer. Cells were washed with Hank's balanced salt solution (HBSS), pre-stained with 20  $\mu$ M DCFDA and rewashed with HBSS two times. Oxidative burst in the stained cells was induced by incubating them in PBS solution containing 100 mM H<sub>2</sub>O<sub>2</sub> for 1 h in CO<sub>2</sub>-incubator. A compound of interest was added to the cells in PBS and incubated for 1 h followed by registration of the fluorescent signal from treated cells on an Infinite M200PRO microplate analyzer (TECAN) at  $\lambda_{\text{ex}}=488$  nm and  $\lambda_{\text{em}}=535$  nm.

## 2.7. Cell viability study

The effect of MPS, TBC-COOH and their mixed micelles on viability of SH-SY5Y and PC-12 cells was evaluated with the aid of an MTT assay. Cells were cultured for 7 h in the presence of compounds, then for 72 h without compounds followed by replacement of the medium with a fresh one containing the MTT reagent (0.5 mg/mL). Cells were additionally cultured for 3 h to allow them to reduce MTT into a water insoluble formazan, which was further dissolved in DMSO (100  $\mu$ L per well). The optical absorbance of formazan solution, which is proportional to the number of viable cells, was measured in each well using an Infinite M200PRO microplate analyzer (TECAN) at a wavelength of 555 nm. The cell



viability was calculated as a percentage of reference cells grown without compounds (100% viability).

## 2.8. HPLC and LC-MS/MS

### 2.8.1. Sample preparation of MPS-treated cells

SH-SY5Y cells were seeded and grown onto a 6-well plate in standard conditions until a confluent monolayer was formed. The medium was then replaced by a fresh one containing 3.1 or 0.6 mg/mL of MPS or its micellar formulations with TBC-COOH (0.5 or 0.1 mg/mL, respectively). The cells were exposed to compounds for 1.5 h in a CO<sub>2</sub>-incubator, during which cells were readily detached from the plate surface. Collected cells were washed two times with chilled HBSS by means of centrifugation. The resultant cell pellet was frozen at -80°C and then lysed in 150 µL solution of 0.1% Triton X100 with 0.1 mM PMSF.

Extraction of MPS and MP was performed according to procedures detailed in [29] with some modifications. The cell lysate was mixed with 400 µL of diethyl ether/dichloromethane (v/v, 60:40). The mixture was agitated at 500 rpm for 15 min at room temperature followed by centrifugation and collection of supernatant (360 µL). The extract was dried on a speed vacuum concentrator, solubilized in 100 µL of dichloromethane/isopropanol mixture (v/v, 85:15) and used for analysis of MPS and MP.

### 2.8.2. LC-MS/MS

Chromatographic separation of glucocorticoids was performed on an Infinity 1290 UHPLC system (Agilent) using Discovery HS C18 column, 3 µm, 5 cm×2.1 mm (Supelco). A triple quadrupole mass-spectrometer QTRAP 6500 (ABSciex) was used as a mass analyzer. Parameters of the analysis were as follows. Electrospray ionization (ESI) was set to the positive ion mode; capillary voltage was 5.2 kV; source type was Turbo Spray Ion Drive with temperature 500°C; curtain gas pressure was 35 psi; declustering potential was 51 V, collision energy was automatically optimized for each transition; flow rate was 0.4 mL/min; injection volume was 5 µL.

MS/MS conditions were optimized using an automated 'Compound optimization' algorithm of the Analyst 1.6.2 software (ABSciex). The mass spectrometric data were analyzed using a MultiQuant 3.0.2 software (AB Sciex). The calibration curve was plotted for analyte concentrations from 0.005 to 500 µM. Data were expressed as mean±SD (n=6).

The statistically significant difference was evaluated by Student's t-test with a significance level of  $p < 0.05$ .

### 3. Results and discussion

#### 3.1. Structure-dependent interaction of block copolymers and glucocorticoids

We studied the linear block copolymers, such as Pluronic L61, L121, F127, and the glycerol-based TBC with their structure and characteristics shown in Fig.1S and Table 1S (SM). The Pluronic copolymers were selected as promising drug carriers studied in anticancer compositions [23,30]. Methylprednisolone (MP), methylprednisolone succinate (MPS) and dexamethasone (DXM) (Fig.1S) were selected as the most frequently used glucocorticoid drugs administered systemically and locally [16].

The compositions of the copolymers and glucocorticoids, prepared by mixing them at different concentrations in aqueous solutions, were assessed with DLS technique. It was found that MPS at a relatively high concentration of 63 mM (31.3 mg/mL) spontaneously rearranges aggregates of some of the copolymers (Pluronic L121, TBC, TBC-COOH). Opaque solutions of these copolymers (5 mg/mL) became transparent after addition of MPS, indicating disappearance of (sub)microsized polymeric aggregates.

To characterize aggregates of the pure copolymers and copolymer-glucocorticoid compositions, the HD, PDI and  $\zeta$ -potential were registered. Average DLS data (mean $\pm$ SD,  $n=3$ ) are summarized in Table 2S (SM). Hydrophobic Pluronic L121 (HLB=1) and the TBC (HLB=3) formed labile thermosensitive aggregates with the HD of over 100 nm (Fig.1A,B, Table 2S). Association of MPS with these copolymers resulted in formation of almost monodisperse small micelles with a mean HD of  $30.0 \pm 0.3$  nm and  $19.0 \pm 0.2$  nm, and a corresponding PDI of 0.1 and 0.2, for Pluronic 121 (Fig.1A, Table 2S) and TBC (Fig.1B, Table 2S), respectively. Furthermore, the composition of carboxylated copolymer TBC-COOH and MPS produced micelles of similar size (HD= $19.6 \pm 0.3$  nm) and higher homogeneity (PDI=0.1) to those of TBC/MPS composition (Fig.1C, Table 2S).

Under the same conditions, no defined particulates were detected for the composition of MPS with Pluronic L61, which possesses relatively low HLB (HLB=3) but poor micelle-forming ability. Relatively hydrophilic Pluronic F127 (HLB=22) with extended polyethylene oxide (PEO) blocks formed a well-defined micellar system with the HD of

23.1±0.04 nm and PDI of 0.1, which however became disorganized in the presence of MPS (Fig.1D, Table 2S).

To reveal the importance of the succinyl group in MPS for the formation of the nanosized micelles, control experiments were performed using non-succinylated glucocorticoids, MP and DXM. Due to their restricted aqueous solubility these glucocorticoids were initially assessed in water/DMSO mixed solvent (1:1 by volume) at a concentration as high as 25 mM. DMSO, however, affected micelle-forming properties of the glucocorticoid compositions with copolymers. To determine potential association of MP and DXM with the copolymers in aqueous solution, the component concentrations were decreased to 0.3 mM (glucocorticoids) and 0.1 mg/mL (TBC-COOH). Both MP and DEX increased homogeneity of the TBC-COOH aggregates, suggesting copolymer-glucocorticoid interactions, but did not assemble into nanosized micelles (Fig.1E) in contrast to MPS, which however was used at a much higher concentration (Figs.1A, 1B, 1C).

Menadione sodium bisulfite (MEN), the water-soluble form of vitamin K (Fig.1S), was additionally studied as a reference compound with an aromatic and anionic structure similar to MPS. Mixing of MEN at a concentration as high as 63 mM with TBC-COOH (5 mg/mL) was also accompanied by disappearance of opalescence of the copolymer solution. DLS analysis showed that the resultant TBC-COOH/MEN composition produces well-defined nanosized aggregates but of a bigger HD (HD=143.2±1.8 nm, PDI=0.2) compared with TBC-COOH/MPS (Fig.2S, SM).

Together, our results reveal that the water-soluble glucocorticoid MPS at increased concentrations associates spontaneously with hydrophobic micelle-forming copolymers of EO/PO into very small and homogeneous mixed micelles. It is likely that MPS binds to the polypropylene oxide (PPO) block of copolymers through its steroid scaffold by means of hydrophobic interaction. This binding presumably requires appropriate physicochemical characteristics of the drug molecule, which relate to its aqueous solubility and anionic nature, including the octanol-water partition coefficient (logP), the distribution coefficient (logD) and the ionization constant (pKa) for ionizable compounds [31]. Decreased logD of MPS (logD is 0.02 at pH 7 [32]) compared with uncharged MP and DXM (theoretical logP is 1.56 and 1.68, respectively, www.drugbank.ca, ChemAxon software) due to the presence of an anionic succinyl group assures amphiphilic properties and sufficient solubility of MPS to allow its self-assembling with the amphiphilic copolymers into mixed micelles.

The fact that MEN (theoretical ACD logD at pH 7.4 is  $-4.55$ ) forms larger and obviously less dense associates with the copolymer under the same conditions shows that MPS possesses more appropriate characteristics, which favor the self-assembly of mixed micelles. These characteristics of MPS, which could relate to its amphiphilic properties, logD, molecular weight, presence of hydroxyl groups, nature and flexibility of the anionic group, should be evaluated elsewhere.

In addition, the  $\zeta$ -potential of the mixed micelles of TBC (TBC-COOH) with MPS and MEN was measured and compared as a criterion for their colloidal stability (Fig.3S, SM). TBC alone produced weakly charged aggregates with  $\zeta$  of  $-0.5 \pm 0.2$  mV, while the TBC-COOH aggregates were anionic with  $\zeta$  of  $-24.2 \pm 4.0$  mV due to the presence of the ionized carboxyl groups. Association of MPS with both TBC and TBC-COOH provided anionic micelles with the  $\zeta$ -potential of  $-24.0 \pm 5.2$  mV for TBC/MPS and  $-27.8 \pm 3.2$  mV for TBC-COOH/MPS (Fig.3S). Interestingly, TBC-COOH/MEN aggregates were characterized by noticeably lower potential of  $-16.2 \pm 1.1$  mV, whereas no micelles were detected for the TBC/MEN composition, suggesting that the copolymer and drug components should provide sufficient anionic charge to stabilize the mixed micelles. These data suggest a type of organization of the mixed copolymer/MPS micelles where the succinate groups of MPS molecules, together with the carboxyl groups and PEO blocks of the copolymer, are oriented into the aqueous phase forming a micellar corona, while the steroid rings of MPS and PPO block of the copolymer form the hydrophobic core ('Graphical abstract').

Among the different copolymers studied, the carboxylated copolymer TBC-COOH was further used to prepare drug formulation, since the TBC-COOH/MPS micelles were characterized by the highest homogeneity and anionic charge. In particular, the  $\zeta$ -potential of TBC-COOH/MPS was almost  $-30$  mV at physiological pH, which generally corresponds to a stable colloidal system [34]. Furthermore, TBC and its derivatives exhibit relatively low adverse effects on mammalian cells compared with hydrophobic Pluronics, and effectively promotes intracellular penetration of small molecules and macromolecules [24,25,33], making them preferable for pharmaceutical applications.

### *3.2. Verification of TBC-COOH/MPS formulation*

#### *3.2.1. Micelle formation at different concentrations of TBC-COOH and MPS*

The quality of the TBC-COOH/MPS micellar system was found to be dependent on concentration (ratio) of the components upon mixing (Fig.4S, SM). When the concentration of MPS was serially diluted from 31.3 to 3.9 mg/mL (concentration of TBC-COOH was 5 mg/mL), the (sub)microsized aggregates were formed, along with the main fraction of the mixed micelles at ~20 nm. These aggregates presumably corresponded to an excess of TBC-COOH or unsaturated copolymer/MPS complexes. Below the MPS concentration of 3.9 mg/mL, the micellar system was disorganized (data not shown). At a constant MPS concentration (31.3 mg/mL), decrease in the TBC-COOH concentration also promoted formation of larger aggregates (Fig.4S). For the given MPS concentration the defined nanosized fraction disappeared at a copolymer concentration below 1.25 mg/mL.

The results show that an optimal weight ratio for the TBC-COOH/MPS micelles according to DLS data is approximately 1:6.3 (copolymer to MPS), which corresponds to ~80 molecules of MPS per one molecule of TBC-COOH and ~1.1 molecules of MPS per each PO unit. This stoichiometry supports chemical affinity of the glucocorticoid drug to the PPO component of the copolymer, which facilitates their self-assembly into the mixed micelles after reaching sufficient constituent concentrations. The disappearance of (sub)micron labile associates upon mixing of TBC-COOH and MPS at the optimal concentrations (31.3 and 5 mg/mL, respectively) (Fig.4S) indicates that the equilibrium is shifted towards the nanosized micelles. These data suggest the possibility of *in situ* preparation of the TBC-COOH/MPS formulation with a relatively high—~~theoretical~~ entrapment efficiency—~~up to 86.3%~~. The structure and stability of the formulation developed were further verified using independent techniques.

### 3.2.2. Interaction of TBC-COOH/MPS with pyrene probe

The TBC-COOH/MPS formulation (weight ratio 1:6.3) was assessed with a pyrene probe which distributes and fluoresces in the hydrophobic milieu of micelles [35]. Fig.5S (SM) shows the dependence of pyrene fluorescence on concentrations of TBC-COOH and TBC-COOH/MPS in PBS. The fluorescent signal of pyrene began to increase at a TBC-COOH concentration of 31  $\mu$ g/mL, reflecting the transition of separate polymeric molecules ('unimers') to their micellar aggregates. Maximum fluorescence was observed at the highest copolymer concentration with an enhancement factor of 4.8 (Fig.5S).

In the case of TBC-COOH/MPS, the fluorescent signal increased at the same TBC-COOH concentration (31  $\mu\text{g/mL}$ ) with an enhancement factor of just 1.7 and decreased at the concentration above 250  $\mu\text{g/mL}$  (Fig.5S). The noticeable decrease in pyrene fluorescence for TBC-COOH/MPS compared with TBC-COOH suggests a suppression of probe/mixed micelle interaction, apparently due to stable occupation of the hydrophobic PPO core by glucocorticoid molecules.

### 3.2.3. Effect of dilution, temperature and blood serum

The dilution effect on micellar stability and structure of the TBC-COOH/MPS formulation was assessed. Fig.2A shows variation of the HD and PDI of the mixed micelles in serial dilution. When TBC-COOH/MPS concentration decreased from 5  $\text{mg/mL}$  to  $\sim 40$   $\mu\text{g/mL}$  for the copolymer (from 31.3 to 0.25  $\text{mg/mL}$  for MPS, respectively), the HD moderately increased from 19.6 to 65 nm. This increase is apparently due to some loosening and swelling of the diluted micelles. Micellar polydispersity increased more significantly under the same conditions (Fig.2A). A further decrease in the concentration of TBC-COOH/MPS (below 40  $\mu\text{g/mL}$  for the copolymer) was accompanied by drastic enlargement of micellar aggregates due to disorganization of the micellar system.

It should be noted that under the same conditions TBC-COOH/MEN aggregates were significantly less stable upon dilution and collapsed at a component concentration of 0.6  $\text{mg/mL}$  (TBC-COOH) and 7.9 mM (MEN) (data not shown). This shows that the TBC-COOH/MPS formulation is relatively stable during dilution.

The thermoresponsive properties of the TBC-COOH/MPS formulation were further estimated. The size of the TBC-COOH/MPS micelles remained unchanged at temperature of 25°C and 37°C (HD=19.6 $\pm$ 0.3 nm), whereas a slight increase in the HD to 21.6 $\pm$ 0.28 nm was observed at 50°C (Fig.2B). These data demonstrate the resistance of TBC-COOH/MPS to thermal fluctuations further supporting its steady micellar structure. This is in great contrast to thermosensitive EO/PO based copolymers which are known to be hydrated and better solubilized at decreased temperatures, while becoming more hydrophobic and susceptible to flocculation at elevated temperatures due to dehydration of the copolymer units [22]. The lack of thermoresponsive properties of the TBC-COOH/MPS formulation suggests decreased sensitivity of the copolymer component to the (de)hydration effect as a result of its association with the glucocorticoid.

Blood serum stability of the formulation was assessed to predict its aggregation in body fluids [36]. For this purpose, TBC-COOH/MPS micelles were analyzed in a model cell culture medium supplemented with 5% FBS (DMEM/FBS). The size of the micellar system in DMEM/FBS remained unchanged (Figs. 1F versus 1C) with only a slight increase in polydispersity (PDI=0.25). This increase in polydispersity is, however, explained by the interfering effect of serum proteins on the DLS analysis. As shown earlier, the size of aggregates of different copolymers of EO and PO alone was significantly affected by serum proteins under the same conditions [27]. The low effect of DMEM/FBS on the mixed micelles is presumably due to decreased adsorption of the serum proteins on the surface of mixed micelles of dense and anionic structure.

#### 3.2.4. AFM of TBC-COOH/MPS formulation

AFM was used to visualize the nanosized TBC-COOH/MPS micelles which were spread and dried onto a surface of freshly cleaved mica (Fig.3). TBC-COOH alone formed large drop-like structures which merged together onto the hydrophilic substrate (Fig.3A), whereas the TBC-COOH/MPS micelles were detected as discrete particulate nanostructures (Fig.3A) with the average dimensions measured at half-height as follows (mean $\pm$ SD): 172.9 $\pm$ 26.2 nm (width) and 40.1 $\pm$ 6.2 nm (height). Further analysis showed that the nanostructures are aggregates, composed of smaller nanoparticles, which are clearly observed in Fig.3B (arrows). These smaller particles with narrower dimensions (width=22.7 $\pm$ 5.7 nm, height=7.8 $\pm$ 2.8 nm) were identified as the TBC-COOH/MPS micelles. Any fluctuations of the geometry may result from shrinking and deformation of the micelles after drying.

The AFM data show that the mixed micelles possess a particulate-like structure which is preserved upon adsorption onto the solid surface. This implies rigidity of the micellar core presumably due to a kind of tight association of MPS molecules with PPO blocks, which is not expected in the case of conventional micellar systems, including liposomes, which generally require more complicated techniques for visualization [10].

Altogether, our results confirm that TBC-COOH and MPS undergo self-assembly to produce uniform and relatively stable mixed micelles. These data support possible usage of the TBC-COOH/MPS as a pharmaceutical formulation. The size and polydispersity of this formulation developed is noticeably lower than those for reported compositions: polysorbate 20/cholesterol vesicles (146-205 nm) [9,10], nanostructured lipid carriers (380-

408 nm) [8], poly(phenylacetylene) and poly(phenylacetylene-co-acrylic acid) nanoparticles (190-500 nm) [37], PLGA nanoparticles (400-600 nm) [17], surfactant-stabilized nanosuspension (300 nm) [13], PLA nanoparticles (345 nm) [15] and microparticles (3.6  $\mu\text{m}$ ) [15]. PEG-PCL micelles loaded with dexamethasone acetate were proposed as an infusion formulation of the low soluble drug [6]. This formulation was characterized by a relatively low drug loading (2-12%) and neutral charge of micelles ( $\zeta$ -potential was  $-1.3$  mV). In addition, these above described formulations require multi-step procedures for their preparation and may contain undesirable toxic solvents and surfactants. The comparison shows substantial advantages of the TBC-COOH/MPS micelles over conventional formulations which rely on entrapment of the glucocorticoid into vehicles rather than self-assembly into uniform mixed micelles. Cellular toxicity and availability of the TBC-COOH/MPS micelles was further assessed as a preliminary part of their pharmacokinetic study.

### 3.3. Effect of TBC-COOH/MPS formulation on cell viability

The effect of the TBC-COOH/MPS micelles on viability of mammalian cells was studied in comparison with the unformulated MPS. In view of possible neuroprotective applications of glucocorticoids, neuronal SH-SY5Y and PC-12 cell lines were used. To better address rapid clearance of MP [38,39], the cells were exposed to the compounds for 7 h, additionally cultured for 72 h and subjected to the MTT assay (section 2.7.). Under these conditions, TBC-COOH did not affect cell viability but promoted cytotoxicity of MPS in the formulation.

Fig.4 shows relationships between cell viability and concentration of MPS and TBC-COOH/MPS. MPS was found to possess a half-maximal inhibitory concentration ( $\text{IC}_{50}$ ) of  $1.0 \pm 0.1$  mg/mL for SH-SY5Y cells and  $1.1 \pm 0.2$  mg/mL for PC-12 cells (mean  $\pm$  SD,  $n=3$ ) due to intrinsic cytotoxicity of the glucocorticoid drugs at the concentration range studied [40,41]. Association of MPS with TBC-COOH led to some decrease in  $\text{IC}_{50}$  value, which was particularly profound for SH-SY5Y cells. The  $\text{IC}_{50}$  of TBC-COOH/MPS was almost  $0.3 \pm 0.1$  mg/mL for SH-SY5Y cells and  $0.9 \pm 0.1$  mg/mL for PC-12 cells in terms of MPS (Fig.4), indicating that the formulated MPS at least preserves its bioactivity *in vitro*.

An almost 3-fold increase in the overall effect of TBC-COOH/MPS on viability of SH-SY5Y cells could be explained by enhanced cellular uptake of the mixed micelles compared



with the unbound glucocorticoid. MPS is considered to have a relatively low permeability across cellular membranes at submillimolar level [42]. Increased diffusion of MPS across the plasma membrane at higher millimolar concentrations seems to promote its cytotoxicity (Fig.4). Entrapment of MPS within the mixed micelles was found to enhance its effect on SH-SY5Y cells predominantly at lower submillimolar range (Fig.4A), which was attributed to improved cellular accumulation of the formulated MPS.

The enhancing effect observed is likely to result from endocytotic uptake of TBC-COOH/MPS micelles, which is typical for polymeric micelles of similar size [43]. These data suggest that association of MPS with TBC-COOH into the mixed micelles increases cellular penetration of the glucocorticoid to different extents depending of a specific cell type.

#### 3.4. Antiradical activity of TBC-COOH/MPS

In view of the established antioxidant activity of MP [44,45], radical-scavenging properties of the formulated MPS were evaluated. A pre-optimized fluorescent assay based on the Fenton-like reaction between  $H_2O_2$  and  $CoCl_2$  was applied as detailed in [46]. The reactive oxygen species (ROS), such as the hydroxyl radical generated in the reaction were detected by using the DCFDA probe.

Fig.5A shows the inhibitory effect of MPS and TBC-COOH/MPS at different concentrations on ROS production in the prooxidant  $CoCl_2/H_2O_2$  reaction. MPS suppressed ROS generation by almost 50% at a concentration as high as 1.6 and 3.1 mg/mL. The inhibitory activity of MPS decreased with concentration in the range from 0.8 to 0.1 mg/mL, where the effect was similar to that of TBC-COOH/MPS. At a concentration of MPS of 3.1 mg/mL, the TBC-COOH/MPS formulation inhibited ROS generation to a much higher extent, namely, almost to 74% value compared with the unformulated MPS (Fig.5A).

These data demonstrate that the TBC-COOH copolymer is capable of promoting the antiradical activity of MPS in the prooxidant reaction (Fig.5A) presumably by diminishing intramolecular interactions of the glucocorticoid and increasing its effective concentration. Reactivity of the formulated MPS seems to be supported by a small size of the mixed micelles and a high molar ratio of MPS to TBC-COOH in the formulation.

*In vitro* antiradical activity of the drug formulations was further assessed on PC-12 cell monolayers in a 96-well microplate format. The cells were pre-stained with DCFDA and

subjected to H<sub>2</sub>O<sub>2</sub>-induced oxidative burst. In addition to MPS, DXM was used for comparison because of its relatively good permeability across cellular membranes [46]. After 1 h exposure, DXM at its upper soluble level of ~0.1 mg/mL (~0.3 mM) was found to decrease cell fluorescence by ~25%, indicating partial inhibition of ROS formation in the cells treated (Fig.5B).

MPS did not significantly affect the fluorescent signal at a 10-fold higher concentration of 1.2 mg/mL (2.5 mM) ( $p < 0.05$ ) which was attributed to its lower intracellular penetration compared with DXM. The antioxidant effect of DXM, however, was only slightly enhanced in the composition with TBC-COOH in contrast to the formulated MPS which exhibited the highest inhibitory action on the oxidative burst by almost 66% (Fig.5B). This enhanced effect of the TBC-COOH/MPS formulation could be explained by its improved cellular uptake compared with DXM and increased reactivity to ROS (Fig.4).

These results highlight a possibility of enhancing antiradical activity of MPS in the composition with TBC-COOH. This effect is of interest in high-dose glucocorticoid therapy of traumatic and ischemic diseases accompanied by intense oxidative stress and inflammation.

### 3.5. Cellular transport of MPS and TBC-COOH/MPS

Analysis of pharmacokinetics of drugs formulations *in vitro* and *in vivo* is an important task. Different mass spectrometry (MS) techniques coupled with gas chromatography [48,49] and liquid chromatography (LC) [50–53] have been proposed to quantify the glucocorticoids in body fluids and tissues. Among them, LC-tandem MS (LC-MS/MS) with triple quadrupole detection and selected reaction monitoring mode is a sensitive technique which is particularly useful for pharmacokinetic applications [54–56]. The detection limits for MP in biological matrices reported were 7.2 ng/mL (plasma) [55], 0.05 ng/g (brain tissue) [53].

The QTRAP 6500 LC-MS/MS system was used to detect intracellular levels of the glucocorticoids after a short-term exposure of SH-SY5Y cells to MPS and TBC-COOH/MPS. Fig.6S (SM) shows the mass spectra of pure MPS as well as its metabolite MP generated upon chemical or enzymatic cleavage of the succinate group [57]. The precursor ion for MPS was registered at 475.1 m/z. According to multiple reaction monitoring (MRM) transition, five ion products of MPS were selected for analysis of the glucocorticoid as

follows (m/z): 321.2 (quantifier), 253.2, 185.0, 161.1, 90.9. The same parameters for MP were as follows (m/z): the precursor ion 375.2, ion products 161.1 (quantifier), 185.0, 135.1, 90.9.

The LC-MS peak area was detected as a signal to quantify the analytes within the concentration range from 5 nM to 500  $\mu$ M (from 2.4 ng/mL to 237  $\mu$ g/mL). Linear relationships between MPS (MP) concentrations (x) and the signal (y) were observed within the range from approximately 0.5 to 250  $\mu$ M with fitted equations being  $y=2.7098\times 10^5x$  ( $r=0.9932$ ) for MPS and  $y=3.8005\times 10^5x$  ( $r=0.9616$ ) for MP. This calibration was far above the detection limit but sufficient for *in vitro* analysis.

Pregrown adhered SH-SY5Y cells were incubated with MPS or TBC-COOH/MPS for 1.5 h at glucocorticoid concentrations of 1.3 and 6.5 mM. Following the incubation, the cells were lysed and the drugs were extracted as detailed in the section 2.8.1. A representative MRM chromatogram of MPS and MP with a retention time of 2.32 and 2.51 min, respectively, is provided in Fig.7S (SM). Fig.6 shows mean intracellular concentrations of MPS and MP as well as total MPS+MP level detected in cell lysates (100  $\mu$ L of lysate of  $10^6$  cells) for two extracellular MPS doses applied.

Both the intracellular level of MPS and MP and their ratio were found to be dependent on the dose applied. At MPS concentration of 6.5 mM, the glucocorticoid was predominantly detected in the cells in its succinylated form (53.1  $\mu$ M and ~89% of the total MPS+MP level), whereas at a 5-fold lower MPS concentration (1.3 mM), the intracellular level of MPS was 9.8  $\mu$ M (~74% of the total MPS+MP level) (Fig.6). Hence, the total intracellular MP concentrations (MPS+MP) for 6.5 and 1.3 mM extracellular MPS doses differed by a factor of ~4.5.

These results indicate that at the doses studied transport of MPS into the cells is controlled by passive diffusion. The intracellular glucocorticoid is predominantly revealed in the esterified form, although some decrease in MPS/MP ratio occurs when extracellular MPS concentration is reduced from 6.5 to 1.3 mM (Fig.6). This is in accordance with observations of the relatively slow intracellular hydrolysis of MPS [42].

No statistically significant difference in the intracellular content of the glucocorticoid was observed for free and formulated MPS at a concentration of 6.5 mM (Fig.6A). Hence, at this concentration, the TBC-COOH/MPS micelles are characterized by the same intracellular uptake as free MPS. At lower MPS concentration of 1.3 mM, an increase in the

glucocorticoid level was observed in the cells treated with the the formulated MPS (Fig.6B). The intracellular glucocorticoid concentration was increased by a factor of 1.52, 1.74 and 1.58 for MPS, MP and MPS+MP, respectively. This increase is consistent with the above presented data on enhanced cytotoxic (Fig.4) and antioxidant activity (Fig.5) of the TBC-COOH/MPS micelles.

Together, our results suggest increased cellular availability of the TBC-COOH/MPS micelles at concentrations of MPS which do not favor drug diffusion across the plasma membrane. Considering the cytosolic and nuclear localization of the glucocorticoid receptors [1], effective intracellular delivery of MPS is prerequisite to its bioactivity.

Our study shows that the TBC-COOH/MPS nanoformulation is characterized by a relatively high availability and activity at molecular and cellular levels (Figs. 4–6). Considering the shown ability of TBC-COOH to enhance permeability of spinal cord tissues [25], we believe that the formulation developed can be used for local delivery of MPS in acute spinal cord injury as well as other traumatic and inflammation-related diseases.

In view of the chemical stability of TBC-COOH in aqueous solution and its self-assembling with MPS, the formulation can be potentially prepared *in situ*, e.g. by mixing lyophilized MPS and presolubilized TBC-COOH in appropriate parenteral forms, such as Solu-Medrol (Pfizer). Our study provides incentive for further preclinical studies into the suitability of the TBC-COOH/MPS nanoformulation for the glucocorticoid therapy.

#### 4. Conclusions

We have, for the first time, developed a uniform and stable micellar formulation of methylprednisolone succinate by its self-assembling with the chemically modified EO/PO copolymer (micelle size=19.6 nm, PDI=0.1,  $\zeta$ = -28 mV). The carboxylated trifunctional block copolymer with improved physicochemical, biocompatible and penetration enhancing properties was used to form mixed micelles, which are characterized by high encapsulation efficacy and cellular availability of MPS. Primary study of the formulation demonstrated its increased cellular uptake and antiradical activity to that of free MPS. LC-MS/MS analysis of cellular transportation and hydrolysis of MPS using QTRAP 6500 system was optimized, which will be further extended for *in vivo* study of the pharmacokinetics of mixed micelles.

#### Acknowledgments

This work was co-funded by Russian Foundation for Basic Researches (Grant No. №16-54-10059\_KO\_a) and performed according to the Russian Government Program of Competitive Growth of the Kazan Federal University. Andrei N. Lukashkin is supported by the Medical Research Council grant [MR/N004299/1] and The Royal Society International Exchanges grant [IE160140]. The equipment was used according to the project of Ministry of Education and Science of the Russian Federation (ID RFMEFI59414X0003). We thank Anna Morozova and Aleksey Rogov (Interdisciplinary Center for Analytical Microscopy, Kazan Federal University) for performing AFM analysis and Ian Russell and George Burwood for their critical reading of early versions of the manuscript.

### Conflict of interest

The authors report no conflict of interest.

### References

- [1] T. Rhen, J.A. Cidlowski, Antiinflammatory action of glucocorticoids - new mechanisms for old drugs, *N. Engl. J. Med.* 353 (2005) 1711-1723.
- [2] D. Annane, E. Bellissant, P.E. Bollaert, J. Briegel, D. Keh, Y. Kupfer, Corticosteroids for severe sepsis and septic shock: a systematic review and meta-analysis, *BMJ* 329 (2004) 480.
- [3] D.J. Short, W.S. El Masry, P.W. Jones, High dose methylprednisolone in the management of acute spinal cord injury - a systematic review from a clinical perspective, *Spinal. Cord.* 38 (2000) 273-286.
- [4] D. Bartholdi, M.E. Schwab, Methylprednisolone inhibits early inflammatory processes but not ischemic cell death after experimental spinal cord lesion in the rat, *Brain. Res.* 672 (1995) 177-186.
- [5] U.I. Tuor, Glucocorticoids and the prevention of hypoxic-ischemic brain damage, *Neurosci. Biobehav. Rev.* 21 (1997) 175-179.
- [6] Y. Wang, M. Wu, L. Gu, X. Li, J. He, L. Zhou, A. Tong, J. Shi, H. Zhu, J. Xu, G. Guo, Effective improvement of the neuroprotective activity after spinal cord injury by synergistic effect of glucocorticoid with biodegradable amphipathic nanomicelles, *Drug Deliv.* 24 (2017) 391-401.
- [7] I.M. Abraham, T. Harkany, K.M. Horvath, P.G. Luiten, Action of glucocorticoids on survival of nerve cells: promoting neurodegeneration or neuroprotection?, *J. Neuroendocrinol* 13 (2001) 749-760.

- [8] S. Doktorovova, J. Araujo, M.L. Garcia, E. Rakovsky, E.B. Souto, Formulating fluticasone propionate in novel PEG-containing nanostructured lipid carriers (PEG-NLC), *Colloids Surf., B* 75 (2010) 538-542.
- [9] C. Terzano, L. Allegra, F. Alhaique, C. Marianecchi, M. Carafa, Non-phospholipid vesicles for pulmonary glucocorticoid delivery, *Eur. J. Pharm. Biopharm.* 59 (2005) 57-62.
- [10] C. Marianecchi, D. Paolino, C. Celia, M. Fresta, M. Carafa, F. Alhaique, Non-ionic surfactant vesicles in pulmonary glucocorticoid delivery: characterization and interaction with human lung fibroblasts, *J. Control. Release* 147 (2010) 127-135.
- [11] D. Triolo, E.F. Craparo, B. Porsio, C. Fiorica, G. Giammona, G. Cavallaro, Polymeric drug delivery micelle-like nanocarriers for pulmonary administration of beclomethasone dipropionate, *Colloids Surf., B* 151 (2017) 206-214.
- [12] R. Iezzi, B.R. Guru, I.V. Glybina, M.K. Mishra, A. Kennedy, R.M. Kannan, Dendrimer-based targeted intravitreal therapy for sustained attenuation of neuroinflammation in retinal degeneration, *Biomaterials* 33 (2012) 979-988.
- [13] H.S. Ali, P. York, A.M. Ali, N. Blagden, Hydrocortisone nanosuspensions for ophthalmic delivery: A comparative study between microfluidic nanoprecipitation and wet milling, *J. Control. Release* 149 (2011) 175-181.
- [14] M.A. Kassem, A.A. Abdel Rahman, M.M. Ghorab, M.B. Ahmed, R.M. Khalil, Nanosuspension as an ophthalmic delivery system for certain glucocorticoid drugs, *Int. J. Pharm.* 340 (2007) 126-133.
- [15] U.B. Kompella, N. Bandi, S.P. Ayalasomayajula, Subconjunctival nano- and microparticles sustain retinal delivery of budesonide, a corticosteroid capable of inhibiting VEGF expression, *Invest. Ophthalmol. Vis. Sci.* 44 (2003) 1192-1201.
- [16] N. El Kechai, F. Agnely, E. Mamelle, Y. Nguyen, E. Ferrary, A. Bochot, Recent advances in local drug delivery to the inner ear, *Int. J. Pharm.* 494 (2015) 83-101.
- [17] D.H. Kim, D.C. Martin, Sustained release of dexamethasone from hydrophilic matrices using PLGA nanoparticles for neural drug delivery, *Biomaterials* 27 (2006) 3031-3037.
- [18] E. Engleder, C. Honeder, J. Klobasa, M. Wirth, Ch. Arnoldner, F. Gabor, Preclinical evaluation of thermoreversible triamcinolone acetonide hydrogels for drug delivery to the inner ear, *Int. J. Pharm.* 471 (2014) 297-302.
- [19] C. Honeder, E. Engleder, H. Schopper, F. Gabor, G. Reznicek, J. Wagenblast, W. Gstoettner, Ch. Arnoldner, Sustained release of triamcinolone acetonide from an intratympanically applied hydrogel designed for the delivery of high glucocorticoid doses, *Audiol. Neurootol.* 19 (2014) 193-202.

- [20] A.N. Salt, J. Hartsock, S. Plontke, C. Lebel, F. Piu, Distribution of dexamethasone and preservation of inner ear function following intratympanic delivery of a gel-based formulation, *Audiol. Neurootol.* 16 (2011) 323-335.
- [21] X. Wang, L. Dellamary, R. Fernandez, Q. Ye, C. Lebel, F. Piu, Principles of inner ear sustained release following intratympanic administration, *Laryngoscope* 121 (2011) 385-391.
- [22] A.V. Kabanov, E.V. Batrakova, V.Y. Alakhov, Pluronic® block copolymers as novel polymer therapeutics for drug and gene delivery, *J. Control. Release* 82 (2002) 189-212.
- [23] E.V. Batrakova, A.V. Kabanov, Pluronic block copolymers: evolution of drug delivery concept from inert nanocarriers to biological response modifiers, *J. Control. Release* 130 (2008) 98-106.
- [24] O.V. Bondar, Y.V. Badeev, Y.G. Shtyrlin, T.I. Abdullin, Lipid-like trifunctional block copolymers of ethylene oxide and propylene oxide: effective and cytocompatible modulators of intracellular drug delivery, *Int. J. Pharm.* 461 (2014) 97-104.
- [25] M.I. Kamalov, I.A. Lavrov, A.A. Yergeshov, Z.Y. Siraeva, M.E. Baltin, A.A. Rizvanov, S.V. Kuznetcova, N.V. Petrova, I.N. Savina, T.I. Abdullin, Non-invasive topical drug delivery to spinal cord with carboxyl-modified trifunctional copolymer of ethylene oxide and propylene oxide, *Colloids Surf., B* 140 (2016) 196-203.
- [26] D. Salakhieva, V. Shevchenko, C. Nemeth, B. Gyarmarti, A. Szilagyi, T. Abdullin, Structure-biocompatibility and transfection activity relationships of cationic polyaspartamides with (dialkylamino)alkyl and alkyl or hydroxyalkyl side groups, *Int. J. Pharm.* 517 (2017) 234-246.
- [27] O.V. Bondar, A.V. Sagitova, Y.V. Badeev, Y.G. Shtyrlin, T.I. Abdullin, Conjugation of succinic acid to non-ionogenic amphiphilic polymers modulates their interaction with cell plasma membrane and reduces cytotoxic activity, *Colloids Surf., B* 109 (2013) 204-211.
- [28] S.L. Hempel, G.R. Buettner, Y.Q. O'Malley, D.A. Welssels, D.M. Flaherty, Dihydrofluorescein diacetate is superior for detecting intracellular oxidants: comparison with 2',7'-dichlorodihydrofluorescein diacetate, 5(and 6)-carboxy-2',7'-dichlorodihydrofluorescein diacetate, and dihydrorhodamine 123, *Free Radic. Biol. Med.* 27 (1999) 146-159.
- [29] P.A. McGinley, J.M. Braughler, E.D. Hall, Determination of methylprednisolone in central nervous tissue and plasma using normal-phase high-performance liquid chromatography, *J. Chromatogr. B Biomed. Sci. Appl.* 230 (1982) 29-35.
- [30] J.W. Valle, A. Armstrong, C. Newman, V. Alakhov, G. Pietrzynski, J. Brewer, S. Campbell, P. Corrie, E.K. Rowinsky, M. Ranson, A phase 2 study of SP1049C, doxorubicin in P-glycoprotein-targeting pluronics, in patients with advanced adenocarcinoma of the esophagus and gastroesophageal junction, *Invest. New Drugs* 29 (2011) 1029-1037.

- [31] S.S. Bharate, V. Kumar, R.A. Vishwakarma, Determining partition coefficient (Log P), distribution coefficient (Log D) and ionization constant (pKa) in early drug discovery, *Comb. Chem. High Throughput Screen.* 19 (2016) 461-469.
- [32] Y. Avnir, K. Turjeman, D. Tulchinsky, A. Sigal, P. Kizelshtein, D. Tzemach, A. Gabizon, Y. Barenholz, Fabrication principles and their contribution to the superior in vivo therapeutic efficacy of nano-liposomes remote loaded with glucocorticoids, *PLOS ONE* 6 (2011) e25721.
- [33] O. Bondar, V. Shevchenko, A. Martynova, D. Salakhieva, I. Savina, Y. Shtyrlin, T. Abdullin, Intracellular delivery of VEGF165 encoding gene therapeutic using trifunctional copolymers of ethylene oxide and propylene oxide, *Eur. Polym. J.* 68 (2015) 680-686.
- [34] D.H. Everett, Basic principles of colloid science, London: The Royal Society of Chemistry (1988) 243.
- [35] D. Wang, Z. Peng, X. Liu, Zh. Tong, Ch. Wang, B. Ren, Synthesis and micelle formation of triblock copolymers of poly(methyl methacrylate)-b-poly(ethylene oxide)-b-poly(methyl methacrylate) in aqueous solution, *Eur. Polym. J.* 43 (2007) 2799-808.
- [36] C.C. Fleischer, U. Kumar, C.K. Payne, Cellular binding of anionic nanoparticles is inhibited by serum proteins independent of nanoparticle composition, *Biomater. Sci.* 1 (2013) 975-982.
- [37] I. Fratoddi, I. Venditti, C. Cametti, C. Palocci, L. Chronopoulou, M. Marino, F. Acconcia, M.V. Russo, Functional polymeric nanoparticles for dexamethasone loading and release, *Colloids Surf., B* 93 (2012) 59-66.
- [38] S.M. Al-Habet, H.J. Rogers, Methylprednisolone pharmacokinetics after intravenous and oral administration, *Br. J. Clin. Pharmacol.* 27 (1989) 285-290.
- [39] P.T. Daley-Yates, A.J. Gregory, C.D. Brooks, Pharmacokinetic and pharmacodynamic assessment of bioavailability for two prodrugs of methylprednisolone, *Br. J. Clin. Pharmacol.* 43 (1997) 593-601.
- [40] C.K. Yeung, K.P. Chan, C.K.M. Chan, C.P. Pang, D.S.C. Lam, Cytotoxicity of triamcinolone on cultured human retinal pigment epithelial cells: comparison with dexamethasone and hydrocortisone, *Jpn. J. Ophthalmol.* 48 (2004) 236-242.
- [41] C.C. Wyles, M.T. Houdek, S.P. Wyles, E.R. Wagner, A. Behfar, R.J. Sierra, Differential cytotoxicity of corticosteroids on human mesenchymal stem cells, *Clin. Orthop. Relat. Res.* 473 (2015) 1155-1164.
- [42] P. Augustijns, P. Annaert, P. Heylen, V. den Mooter, R. Kinget, Drug absorption studies of prodrug esters using the Caco-2 model: evaluation of ester hydrolysis and transepithelial transport, *Int. J. Pharm.* 166 (1998) 45-53.



- [43] Y. Kim, M.H. Pourgholami, D.L. Morris, H. Lu, M.H. Stenzel, Effect of shell-crosslinking of micelles on endocytosis and exocytosis: acceleration of exocytosis by crosslinking, *Biomater. Sci.* 1 (2013) 265-275.
- [44] E.D. Hall, The neuroprotective pharmacology of methylprednisolone, *J. Neurosurg.* 76 (1992) 13-22.
- [45] E. Kaptanoglu, M. Tuncel, S. Palaoglu, A. Konan, E. Demirpence, K. Kilinc, Comparison of the effects of melatonin and methylprednisolone in experimental spinal cord injury, *J. Neurosurg. Spine* 93 (2000) 77-84.
- [46] R.A. Akhmadishina, E.V. Kuznetsova, G.R. Sadrieva, L.R. Sabirzyanova, I.S. Nizamov, G.R. Akhmedova, I.D. Nizamov, T.I. Abdullin. Glutathione salts of O,O-diorganyl dithiophosphoric acids: Synthesis and study as redox modulating and antiproliferative compounds, *Peptides* (2017) <https://doi.org/10.1016/j.peptides.2017.10.002>.
- [47] G. Camenisch, J. Alsenz, H. van de Waterbeemd, G. Folkers, Estimation of permeability by passive diffusion through Caco-2 cell monolayers using the drugs' lipophilicity and molecular weight, *Eur. J. Pharm. Sci.* 6 (1998) 313-319.
- [48] K. Shimada, K. Mitamura, T. Higashi, Gas chromatography and high-performance liquid chromatography of natural steroids, *J. Chromatogr. A* 935 (2001) 141-172.
- [49] L. Amendola, F. Garribba, F. Botre, Determination of endogenous and synthetic glucocorticoids in human urine by gas chromatography-mass spectrometry following microwave-assisted derivatization, *Anal. Chim. Acta.* 489 (2003) 233-243.
- [50] V. Cirimele, P. Kintz, V. Dumestre, J.P. Gouille, B. Ludes, Identification of ten corticosteroids in human hair by liquid chromatography-ionspray mass spectrometry, *Forensic Sci. Int.* 107 (2000) 381-388.
- [51] C.G. Georgakopoulos, A. Vonaparti, M. Stamou, P. Kiouisi, E. Lyris, Y.S. Angells, G. Tsoupras, B. Wuest, M.W.F. Nielen, I. Panderi, M. Koupparis, Preventive doping control analysis: liquid and gas chromatography time-of-flight mass spectrometry for detection of designer steroids, *Rapid Commun. Mass Spectrom.* 21 (2007) 2439-2446.
- [52] R. Mehvar, R.O. Dann, D.A. Hoganson, Simultaneous analysis of methylprednisolone, methylprednisolone succinate, and endogenous corticosterone in rat plasma, *J. Pharm. Biomed. Anal.* 22 (2000) 1015-1022.
- [53] P.J. Gaillard, C.C.M. Appeldoorn, J. Rip, R. Dorland, S.M.A. van der Pol, G. Kooij, H.E. de Vries, A. Reijkerkerk, Enhanced brain delivery of liposomal methylprednisolone improved therapeutic efficacy in a model of neuroinflammation, *J. Control. Release* 164 (2012) 364-369.

- [54] R.L. Taylor, S.K. Grebe, R.J. Singh, Quantitative, highly sensitive liquid chromatography-tandem mass spectrometry method for detection of synthetic corticosteroids, *Clin. Chem.* 50 (2004) 2345-2352.
- [55] R. Difrancesco, V. Frerichs, J. Donnelly, C. Hagler, J. Hochreiter, K.M. Tornatore, Simultaneous determination of cortisol, dexamethasone, methylprednisolone, prednisone, prednisolone, mycophenolic acid and mycophenolic acid glucuronide in human plasma utilizing liquid chromatography-tandem mass spectrometry, *J. Chromatogr. B. Analyt. Technol. Biomed. Life. Sci.* 859 (2007) 42-51.
- [56] M.J. Bueno, A. Aguera, M.J. Gomez, M.D. Hernando, J.F. Garcia-Reyes, A.R. Fernandez-Alba, Application of liquid chromatography/quadrupole-linear Ion trap mass spectrometry and time-of-flight mass spectrometry to the determination of pharmaceuticals and related contaminants in wastewater, *Anal. Chem.* 79 (2007) 9372-9384.
- [57] R. Mehvar, R.O. Dann, DA. Hoganson, Kinetics of hydrolysis of dextran-methylprednisolone succinate, a macromolecular prodrug of methylprednisolone, in rat blood and liver lysosomes, *J. Control. Release* 68 (2000) 53-61.

### Figure captions

**Fig. 1.** Representative distributions of the hydrodynamic diameter of block copolymers and their compositions with glucocorticoid drugs. (A) Pluronic L121, (B) trifunctional block copolymer (TBC), (C, E, F) TBC-COOH, (D) Pluronic F127. (A–D), (F) methylprednisolone succinate (MPS), (E) methylprednisolone (MP), dexamethasone (DXM). (○) pure copolymer solution; (□) copolymer/glucocorticoid composition. Concentrations (A–D), (F): copolymers 5 mg/mL, MPS 31.3 mg/mL, (E): all components 0.1 mg/mL.

**Fig. 2.** (A) Relationships between (○) hydrodynamic diameter (HD), (□) particle dispersion index (PDI) of TBC-COOH/MPS micelles upon serial dilution. Initial concentrations: TBC-COOH 5 mg/mL, MPS 31.3 mg/mL. The critical concentration for disruption of the micellar system is indicated by the vertical arrow. (B) Effect of temperature on HD of TBC-COOH/MPS micelles.

**Fig. 3.** Atomic force microscopy images of (A) TBC-COOH and (A, B) TBC-COOH/MPS micelles spread onto mica surface. The discrete micelles (left column, arrows) and their height profile (right column) are shown in (B).

**Fig. 4.** Concentration–cell viability curves for (○) methylprednisolone succinate (MPS) and (□) TBC-COOH/MPS micelles. SH-SY5Y and PC-12 cells were pre-cultured with compounds for 7 h followed by MTT assay (72 h). The micelles were prepared at 1:6.3 weight ratio; starting concentration of MPS in the medium is 5 mg/mL. The data were fitted using ‘dose response/sigmoidal’ function (OriginPro 8 software)  $y=A1+(A2-A1)/(1+10^{((IC_{50}-x)*p)})$ , where y is viability (%), x is MPS concentration, A1 is the bottom asymptote, A2 is the top asymptote (limited to 100%),  $IC_{50}$  is the half-maximal inhibitory concentration, p is Hill slope. R-squared for the fit is 0.99 and 0.71 for SH-SY5Y and 0.93 and 0.96 for PC-12 cells for MPS and TBC-COOH/MPS, respectively.

**Fig. 5.** Inhibitory effect of glucocorticoids and TBC-COOH/glucocorticoid compositions on  $H_2O_2$ -induced generation of oxygen radicals (A) in cell-free reaction with cobalt chloride and (B) in treated PC-12 cells. For (A), 100% corresponds to Co/ $H_2O_2$  reaction without effectors. TBC-COOH/MPS micelles were prepared at 1:6.3 weight ratio. For (B), 1 – control ( $H_2O_2$ -treated cells without effectors), 2 – MPS, 3 – DXM, 4 – TBC-COOH/MPS, 5 – TBC-COOH/DXM. Concentrations (mg/mL): 1.2 (MPS), 0.1 (DXM), 0.2 (TBC-COOH). Mean±SD (n=3) are shown. Oxygen radicals were detected by using DCFDA probe; DCFDA-stained PC-12 cells were incubated with drug formulations for 1 h.

**Fig. 6.** Concentration of methylprednisolone succinate (MPS) and methylprednisolone (MP) in extract of SH-SY5Y cells exposed to MPS and TBC-COOH/MPS micelles at MPS concentrations of (A) 6.5 mM; (B) 1.3 mM. Mean±SD are shown, \*p<0.05, n=6,  $\sim 10^6$  cells per 100  $\mu$ L of extract.

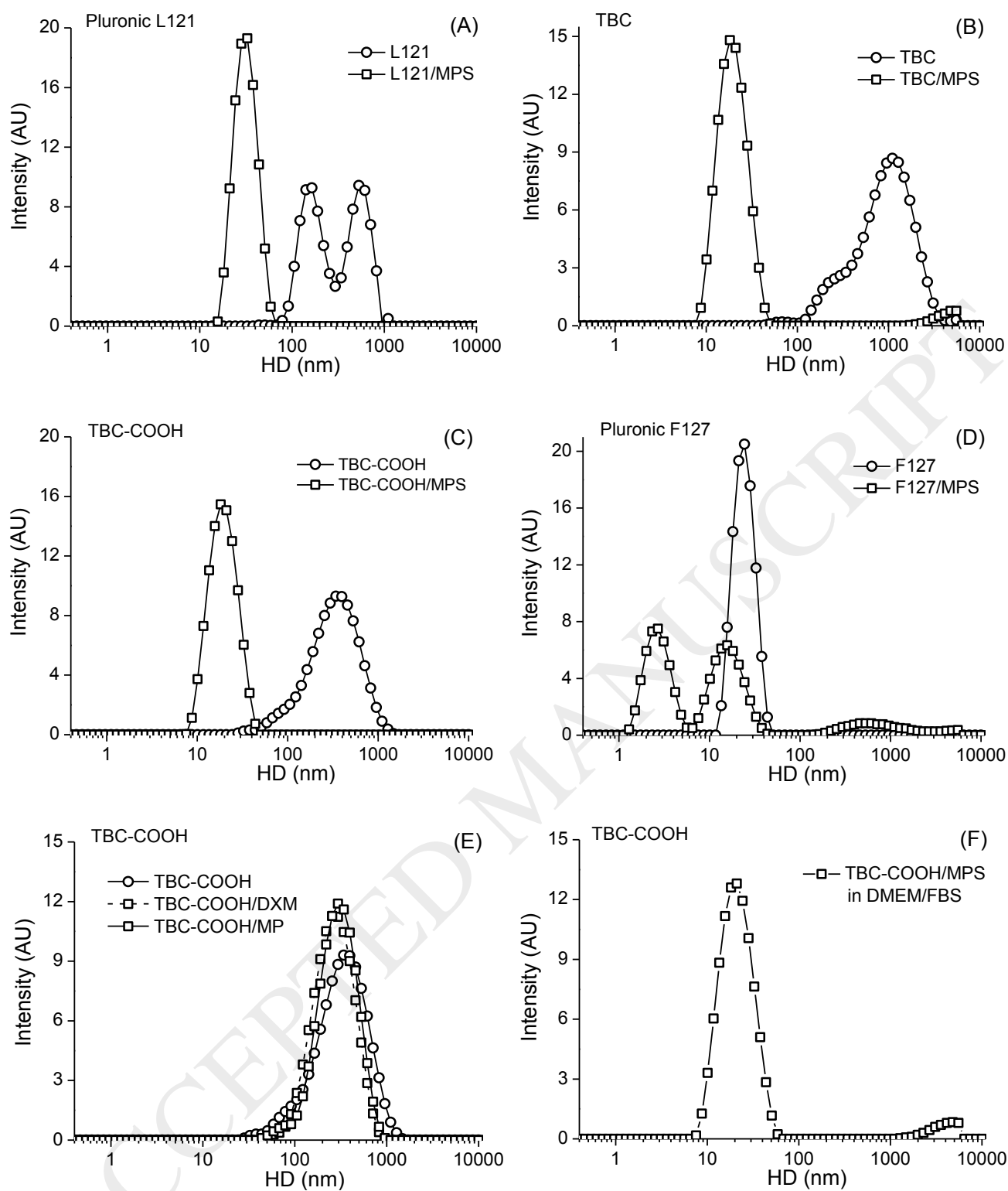


Fig. 1

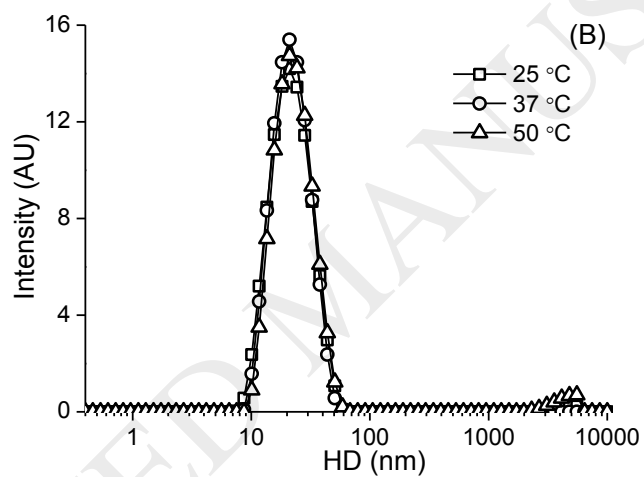
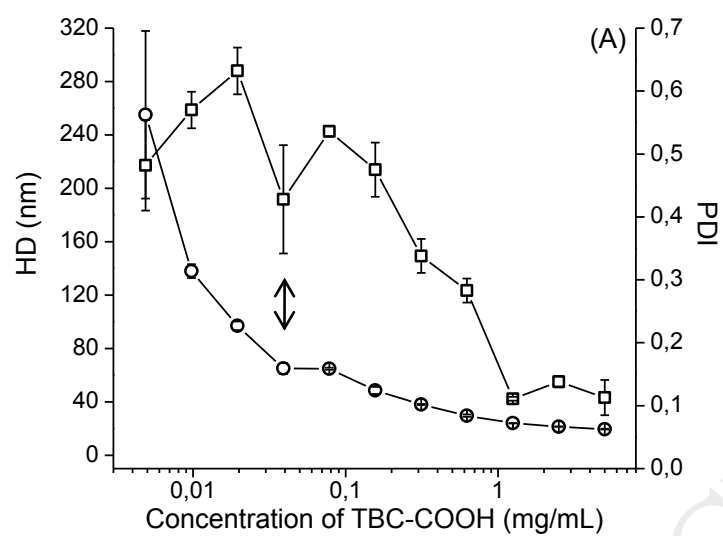


Fig. 2

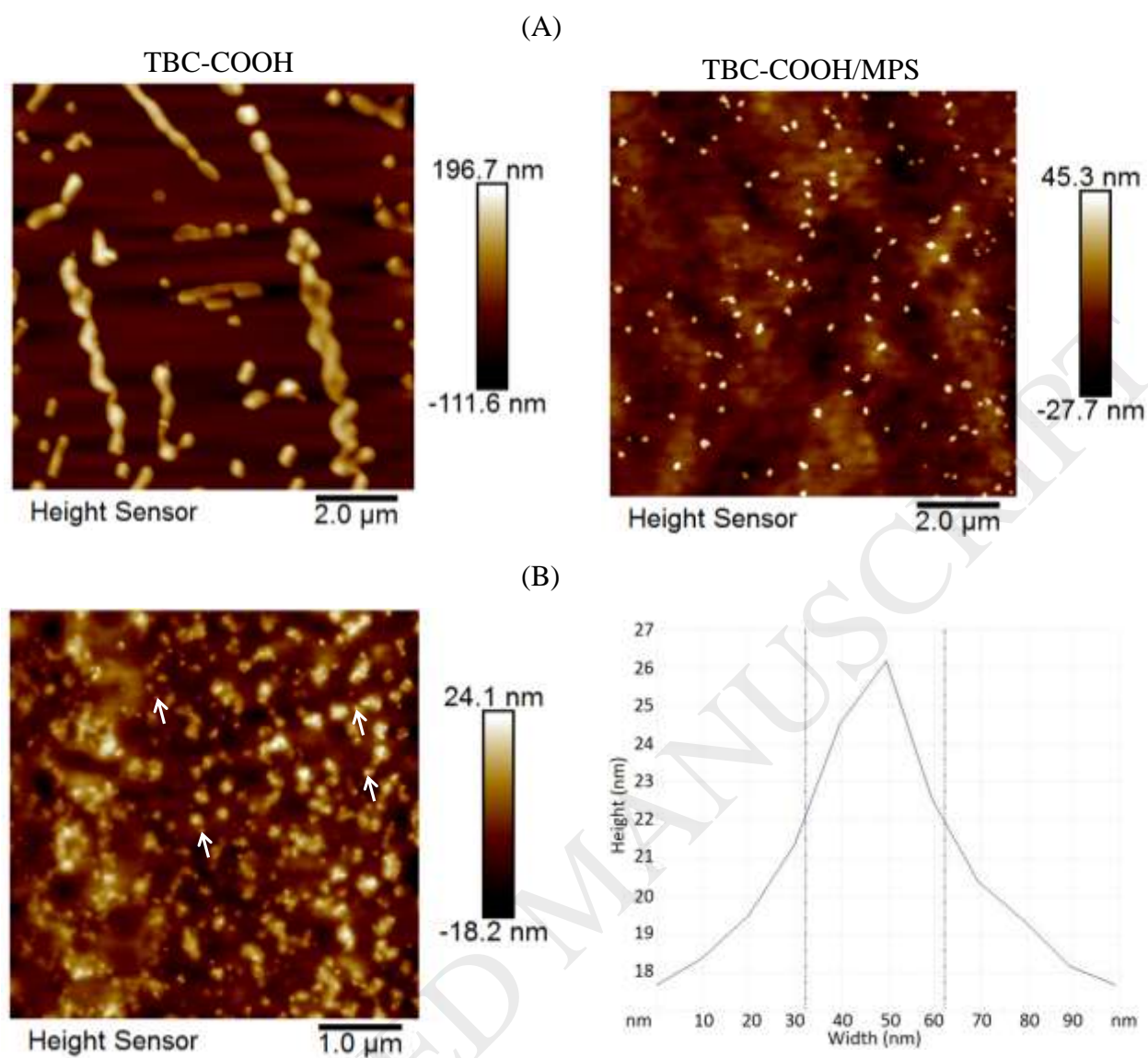


Fig. 3

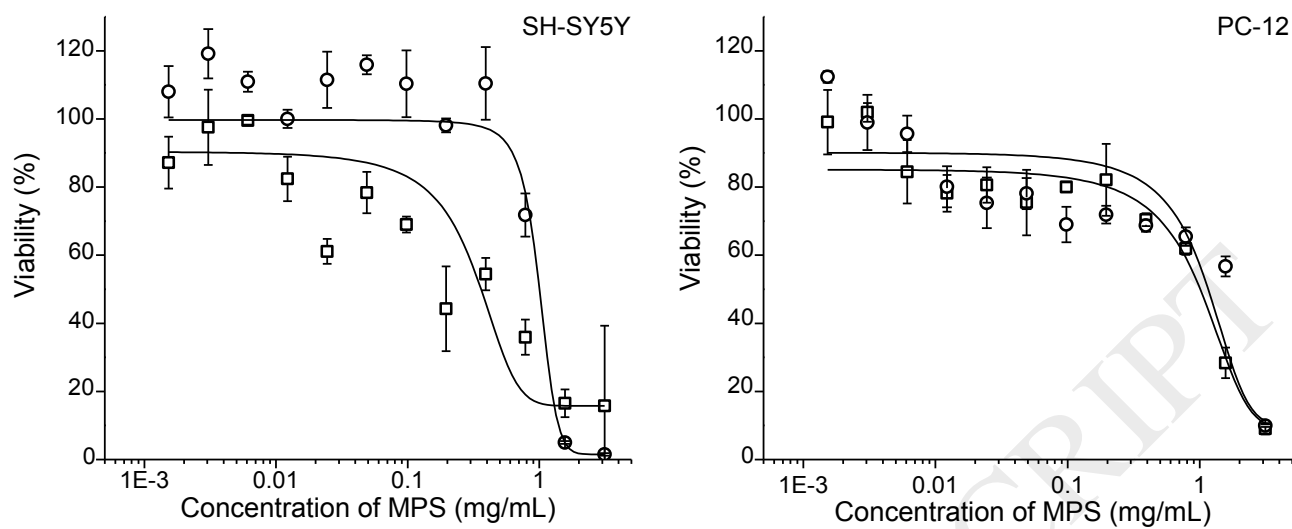


Fig. 4

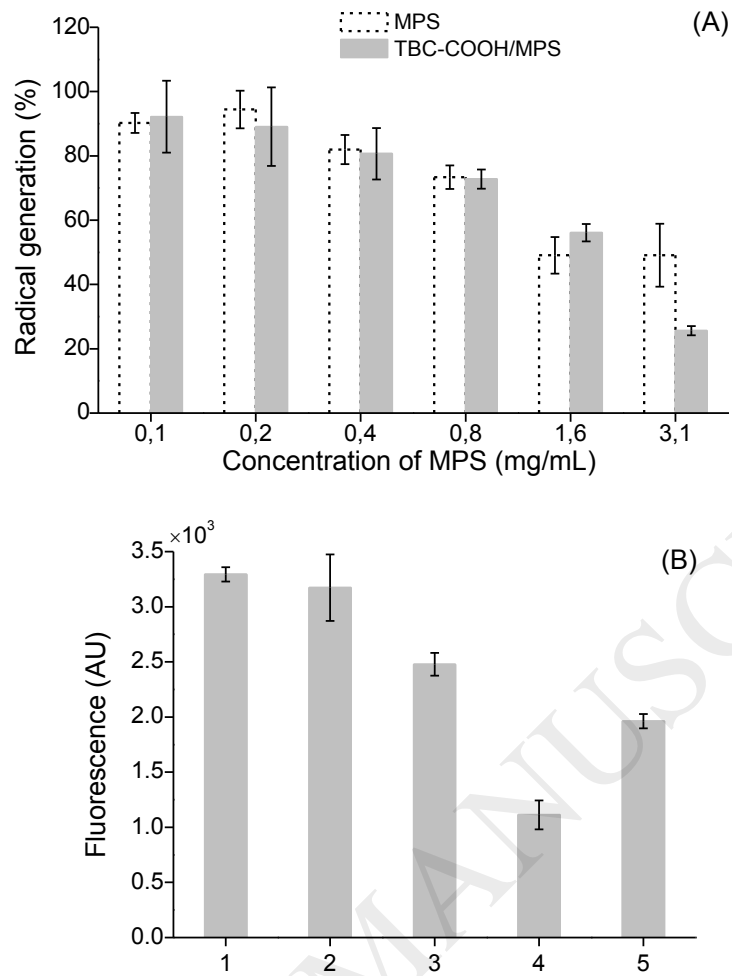
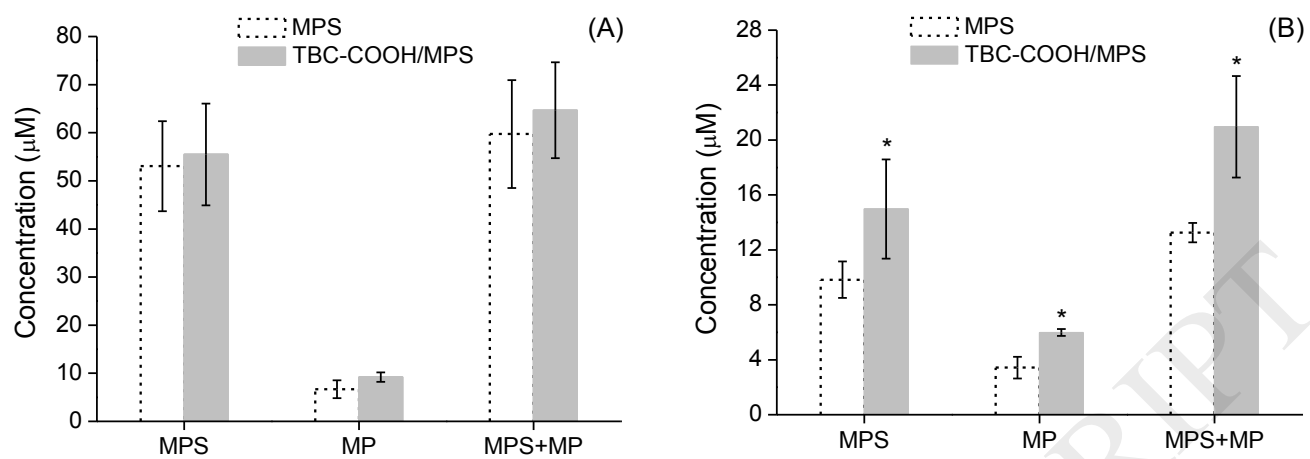


Fig. 5



**Fig. 6**